

Experimental Measurements on the Characteristics of
Flow Transport, Pressure Drop and Jet Impact on
Thermal Insulation

report prepared by

D. R. Williams, Ph.D.

Associate Professor of Mechanical Engineering

Illinois Institute of Technology

Chicago, Illinois

for

TRANSCO PRODUCTS INC.

Chicago, Illinois

May 18, 1992

9404070227 940303
PDR DRG NREA
PDR

Abstract

Experiments were conducted on samples of insulation materials verified as Thermal Wrap[®] provided by Transco Products, Inc. to determine the transport, jet impact, buoyancy and pressure drop characteristics that could play a role following a loss of coolant accident in a nuclear power plant. The measurement techniques were guided by those described in TTS-9103N Rev 1.0. Although the dimensions of the water flume and buoyancy facilities were slightly smaller than those listed in TTS-9103, the tests were not biased by the limitations. The measurements involved determining the speed of water at which the insulation would begin to be transported toward a sump screen, and the speed at which the insulation flips up on the screen. Simple buoyancy tests were made to determine the rate that the insulation would sink. The pressure drop was measured across various thicknesses of thermal insulation in various configurations (as-fabricated, fragments and shreds) simulating debris from a loss-of-coolant accident. The long term effects of temperature and pH = 9.5 on the head loss characteristics were studied. Measurements of the stagnation pressure required for a high-pressure water jet to break through the cover of a standard insulation pillow were also made. Compressibility of the insulation and water temperature were found to have a significant effect on the pressure drop.

1.0 Introduction

Following the issue of Regulatory Guide 1.82 by the Nuclear Regulatory Commission in 1985, it became necessary for operators of nuclear power plants to ensure the ECC sumps and pump inlets can provide sufficient flow rates following a loss-of-coolant accident (LOCA). In the unlikely event of such an accident, there is the possibility that the thermal insulation covering various piping and equipment in the containment building would be dislodged. If the insulation were to find its way to the trash racks and sump screens preceding the ECC pumps, then the flow rates through the ECC sump pumps could be reduced. Clearly, some reliable estimates under a worst case scenario need to be computed. To this end, test procedures to determine various characteristics of the thermal insulation have been described in the test specification TTS-9103N, Rev. 1.

Two types of insulation (series A and series B)¹ and four pillows of each insulation type were supplied for testing by Transco Products, Inc.

2.0 Transport Tests

The scenario for a loss-of-coolant accident assumes piping in the containment building will rupture, and high pressure jets will distribute the thermal insulation in various sizes throughout the containment building. The insulation debris that sinks to the floor may be transported toward the sump screens by the ECC sump suction flow. A reasonable estimate of the flow rate required for the debris to begin moving allows for the identification of the insulation debris having

¹ Series A - Thermal Wrap © Insulation Type 'K'
Series B - Thermal Wrap © Insulation Type 'O'

the potential to collect on the ECC sump screens. The flow speed at which insulation first begins to move is called the "transport speed".

Once the insulation reaches the sump screen, it is possible for the flow to lift up the insulation, so that it "flips-up" on to the screen. This speed is the "flip-up" speed. Both flow rates were determined by testing various samples in a recirculating water flume.

2.1 Test Facility

The transport tests were conducted in a recirculating water channel (flume) located in room 028 of the Engineering-1 Building at the Illinois Institute of Technology. The test section of the flume was 8 ft. long, 4 ft. wide with a water depth of 6 inches. The water temperature was maintained at 15 ± 0.5 °C. The flow speed was controlled by two valves, and could be varied from 0 to 1.0 ft/s. The bottom of the test section was a glass plate.

A 1/16 in. perforated plate with 0.25 in. diameter holes and a 52% open area was used to simulate the sump screen. The plate was bent into a 8 in. x 8 in. L-shape, then was placed at the downstream end of the test section of the water flume.

2.2 Test Results

Two types of thermal insulation (series A and series B) and four pillows of each insulation type were supplied by Transco Products. The samples tested were in a variety of different shapes and sizes as listed in Tables 1 and 2. In order to determine the flow speed necessary to transport the material, it was first necessary to remove all the air so it would sink to the bottom of the test section. The slightest amount of air caught between the layers of the insulation would create sufficient buoyancy for the piece to float. The water temperature in the flume was too low for the insulation to sink on its own, so it was necessary to manually press the air out. It

is believed that many of the glass fibers that make up the insulation are fractured and broken when the air is manually pressed out. This has the effect of accelerating the "aging" of the insulation materials, both with respect to the installed condition, as well as when it is collected on the ECC sump screen during flow.

Once the piece rested on the bottom of the test section, the pump was started, and the flow speed was slowly increased until the sample began to move along the plate. Occasionally the sample would move a short distance then stop. The flow speed would be increased by a small amount until the sample moved without stopping. This defined the "transport speed."

It is important to understand the physics of the transport process. The sample will begin to move when the drag force of the flow around the sample exceeds the frictional resistance of the sample against the floor of the test section. Since the test section was a smooth glass plate, it is clear that the coefficient of friction is much lower than if the sample were placed on a concrete floor. Therefore, the transport speeds listed in Tables 1 and 2 should be considered conservative.

The flow velocity measurements were obtained by marking the fluid with dye and timing its motion over a 25 in. length. The repeatability of velocity measurements with such a technique was 2.6 percent. The transport velocity measurements were repeated at least twice for each sample tested. The repeatability of the onset of motion for the samples was determined to be 6.3 percent.

The results for tests on series A, series B, and four pillows of each type insulation are shown in Tables 1 and 2. The data show the average flow speeds obtained for all the tests performed on each sample. In some cases the sample could be oriented in two directions with respect to the oncoming flow. For example, the 24 x 3 x 3 could be positioned with the longest side perpendicular to the flow

(labeled as horiz.) or aligned with the flow direction (labeled as long.). It was clear that aligning the piece with the flow direction produced a more "streamlined" shape with a lower drag coefficient, so the transport speed was much larger than for the same piece oriented perpendicular to the flow. Tests on the complete pillows of insulation showed transport speeds significantly larger than the bare insulation. This can be attributed to a higher coefficient of friction between the cover and the glass plate, and possibly a higher weight for a specific sample size.

In general the flip-up speeds were larger than the transport speeds. The shape of the sample had a large effect on the flip-up speed. If the height-to-width ratio of the sample was 1:1 then it would not flip-up on to the screen. Typically, lower flip-up speeds occurred when the sample was wider relative to its height. Because the water depth was limited to 6 in., it was not possible to accurately measure the flip-up speed for some of the larger samples. These cases have been indicated with n/a in Table I. Some other cases have been labelled as "will not flip up". When these samples reached the sump screen they remained flat on the bottom of the water flume, even at the highest flow speed.

Table 1 - Series A Transport Tests

T = 15 °C

Size (inches)	Transport Speed	Flip-up Speed	Comments
24 x 3 x 3 (horiz)	0.12		will not flip-up
24 x 3 x 3 (long)	0.38		n/a
24 x 3 x 2.5 (horiz)	0.15	0.17	
24 x 3 x 1.5 (horiz)	0.18	0.23	
12 x 12 x 1	0.14		will not flip-up
6 x 6 x 2	0.15	.52	
6 x 6 x 1	0.13	0.38	
4 x 4 x 3	0.15	0.80	
4 x 4 x 2	0.18	0.70	
3 x 3 x 3	0.24		will not flip-up
3 x 3 x 1.5	0.24		will not flip-up
3 x 3 x 1	0.17		will not flip-up
3 x 3 x 2.5	0.21	0.29	
3 x 3 x .75	0.15	0.30	
3 x 1 x 1 (horiz)	0.18	0.20	
3 x 1 x 1 (long)	0.36	0.28	
1 x 1 x 0.125	0.16	0.39	
TW-A1-2 (pillow)	.51		n/a
TW-A1-3 (pillow)	.44		n/a

Table 2 - Series B Transport Tests

T = 15 °C

Size (inches)	Transport Speed	Flip-up Speed	Comments
24 x 24 x 3	.32		n/a
24 x 24 x 2	.31		n/a
24 x 3 x 3 (horiz)	.075		will not flip-up
24 x 3 x 1.5 (horiz)	.131	.18	
24 x 3 x 3 (long)	.4		will not flip-up
12 x 12 x 2	.25		n/a
12 x 12 x 0.5	.32		n/a
6 x 6 x 2	.28	.41	
6 x 6 x 0.5	.25	.33	
4 x 4 x 3	.30		will not flip-up
4 x 4 x 2	.26		will not flip-up
3 x 3 x 3	.21		will not flip-up
3 x 3 x 2	.22		will not flip-up
3 x 3 x 1.5	.22		will not flip-up
3 x 3 x 1	.17	.28	
3 x 3 x 0.5	.18	.125	
3 x 1 x 1 (horiz)	.13		will not flip-up
3 x 1 x 1 (long)	.31		will not flip-up
1 x 1 x 0.125	.22	.33	
TW-B1-2	.56		n/a
TW-B1-3	.38		n/a

3.0 Buoyancy Tests

Assuming that an insulated pipe were to rupture during a loss-of-coolant accident, the associated insulation will fall onto the free surface of the water collected in the containment building. The rate that the insulation sinks will determine how fast insulation is collected on the floor. The transport speed of the insulation would be close to the flow speed while the insulation is in a buoyant state. Material that does not sink will not have a chance to collect on the ECC sump screens, and should not affect the ECC water system. Tests were conducted on a number of different sample shapes and sizes to determine their buoyancy characteristics.

3.1 Test Facility

The experiments were conducted in a cylindrical stainless steel tank that was 31 in. in diameter and 36 in. deep. A shower head was located in the center of the tank cover to spray the insulation with water. The water depth was set at 18 in. The drain was located in the center of the bottom of the tank, and was connected to a recirculating water pump. A water heater was used to maintain constant temperature. Tests were conducted at room temperature, at 53 °C (128 °F) and 76 °C (169 °F). The water temperature was measured with an Omega model 450 thermocouple.

3.2 Results

The following samples were tested.

- 1) TW-A1-3 pillow
- 2) TW-B1-3 pillow

- 3) 1/8 x 1/8 x 1 shreds, series A and series B
 - 4) 1 x 1 x 1 fragments, series A and series B
 - 5) 3 x 4 x 1/8 shred, series A and series B
 - 6) 4 x 4 x 2 sample, series A and series B
 - 7) 6 x 6 x 2 sample, series A and series B
- (all dimensions in inches)

Each sample was placed on the water surface without forcing any air out of it. In each case the spray of water from the shower head soaked the top of the insulation. In the room temperature experiments and at 53 °C the spray caused air to be trapped inside the insulation. Once the air was trapped, the sample would only sink partially below the surface. The pillows also trapped air and would not sink. After 7 hours of exposure the pillows were removed and the small samples were placed in the tank. Only after 10 days of immersion, the smallest sample, (shreds and fragments) sank. The larger samples (#6, #7) decomposed into layers of different sizes. Approximately half of the layers would lose their air and sink, while the other half would continue to float.

Different behavior was observed in the high temperature test at 76 °C. All samples (including the pillows) sank over a relatively short period of time. The shreds and fragments would not trap air, and all samples sank on contact with the water. The largest samples absorbed the water rapidly and sank within a few seconds of contact with the water. This occurred even with the spray of water turned off. The pillow TW-A1-3 floated for 25 minutes before sinking, while the pillow TW-B1-3 sank within 5 minutes.

The strong dependence of the water viscosity on temperature is believed to be responsible for the change in buoyancy times with temperature. At higher temperature the decreasing viscosity allows the water to flow through the porous

insulation much faster than at low temperatures. Trapped air pockets were never observed to form in the high temperature experiments.

4.0 Head Loss Measurement

In the event that the insulation dislodged from the piping and equipment sinks to the floor of the containment building and is transported by the flow to the ECC sump screens, then the blockage by the insulation will reduce the flow rate through the ECC water system. It is important to have an accurate measure of the head loss characteristics across the different types of insulation in order to be able to predict the flow rates associated with the accumulation of insulation on the ECC sump screens. Because the insulation subject to LOCA forces would have a wide range of shapes and sizes, three different shapes of material were tested for both series A and series B samples.

- 1) "as-fabricated" - material cut from the 24 x 24 x 2 panels to fit the test section
- 2) fragments - sample material cut into 1 x 1 in. squares
- 3) shreds - material cut into 1/4 x 1/4 squares.

Various thicknesses were obtained by building up the layers into the desired thickness.

The shreds were meant to simulate the debris generated by high-pressure jet impingement on the insulation that would occur within 3 diameters of the break in the pipe (region I destruction.) The fragments represent the damage level that occurs farther from the pipe break ($3 < L/D < 7$, region II destruction.) The "as-fabricated" samples correspond to region III destruction ($L/D > 7$) where large sections of insulation are dislodged from the pipe without much damage to the panels.

The purpose of the following tests is to determine the head loss across the various samples of insulation, and to determine the values of the coefficients a, b

and c for the formula $\Delta h = ae^{bv^c}$, where Δh is the head loss in feet of water, e is the nominal thickness in feet, and v is the flow speed in ft/sec.

4.1 Test Facility

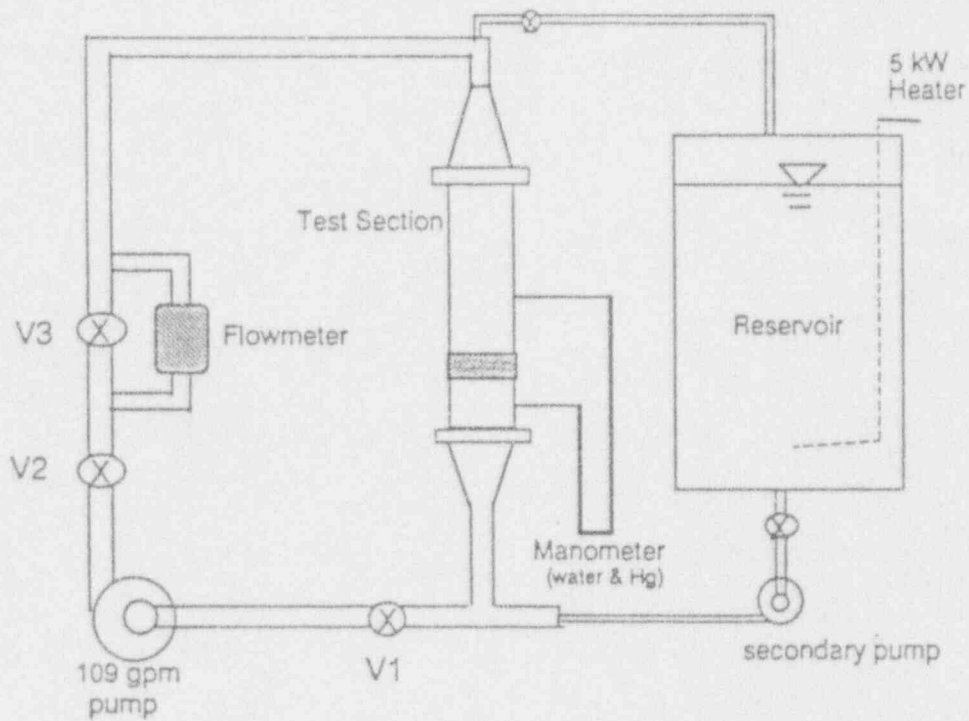


Figure 1. Schematic of Pipe Flow Test Facility

The main element of the facility to measure pressure drop consists of an 8" diameter clear Plexiglas pipe section. The length of the test section is 52 inches. The facility is driven by a 109 gpm pump with a 3 HP electric motor. All piping in the main loop was 4 inch schedule 80 PVC. The flow rate was controlled by valves V1 and V2, and could be varied from 0 to 0.7 ft/sec.

A secondary flow loop was added to the primary system which allowed the water to be conditioned (pH adjusted) and heated. A 100 gallon reservoir was heated with a 5kW electric heater. Temperatures up to 85 °C could be reached in the reservoir, but to avoid damaging the Plexiglas pipe, the system temperature was kept below 60 °C. Various chemicals were added to the reservoir to change the pH level of the water. Borax was added until the pH reached 9.5. This was buffered with a small amount of Sodium hydroxide. A Hanna pH meter was used to measure the system pH, and was calibrated against known pH standards.

The flow rate through the facility was measured with a TVP fluidic-oscillator. The pipe flow system was calibrated by injecting small amounts of dye into the test section and measuring the time for the dye to traverse a 21 inch length. The frequency of the fluidic oscillator was measured with a Hewlett Packard spectrum analyzer over a flow rate range from 0.05 ft/s to 0.6 ft/s. The overall uncertainty in the velocity measurements based on the repeatability of the calibration was 2 percent of the reading.

Nominal insulation thicknesses (e) of 0.125, 0.25, 0.50, 1.0, 2.0, 3.0 and 6.0 inches were tested. The term "nominal" refers to the thickness of the dry insulation in its fabricated state. After the insulation was cut into small fragments (1 x 1 inch squares) or shreds (1/4 x 1/4 inch squares), and placed into the pipe, then the measured initial thickness (l_0) would be significantly larger than the nominal

thickness. The difference in the thicknesses is due to the voids between the spaces created by the random orientation of the fragmented glass fibers. When the flow was turned on in the pipe, then the insulation would be compressed to a smaller thickness (1).

Pressure taps were placed 21 inches above and 13 inches below the screen that held the insulation in place. At each height four pressure taps were placed around the azimuth of the pipe to provide an average pressure at that location. The upper and lower sets of pressure taps were connected to either a mercury manometer or a water manometer depending on the magnitude of the head loss across the insulation. The water manometer was used when the head loss was less than two feet.

4.2 Discussion

In general the "as-fabricated" insulation has the largest head loss, the shreds are intermediate and the fragments have the lowest head loss for a specified flow speed, thickness and temperature. It is apparent that the size of the voids in the material play a major role in the head loss. For example, the fragments show the lowest pressure drop, because the voids created by their random orientation is the largest. As the flow speed increases the material is compressed, which decreases the size of the voids and increases the head loss.

The dependence of the data on the thickness and the flow rate for series A and B can be seen in Figures 2-7. In all cases shown, the insulation was preconditioned (air was manually pressed out) by soaking the samples in water before installing it in the test section. The purpose was to avoid inaccurate measurements of head loss due to trapped air in the insulation. However, the "preconditioning" has the adverse effect of breaking fibers and reducing the size of

the pathways available for the water to flow through the insulation, which results in a higher pressure drop than would be experienced with newly deposited insulation debris immediately following the LOCA accident. Thus the preconditioning simulates extended exposure to the flow and imposes increased conservatism in the results.

To test the idea that preconditioning reduces the size of the "voids" available for the flow to pass through the insulation, a 6 inch (nominal) thickness of dry series A shreds was placed inside of the test pipe. The pipe was slowly filled to avoid any damage or compression of the shreds. A small percentage of the insulation sank, but the majority floated at the top of the pipe until the pump was started and the flow convected the insulation toward the sump screen. The flow was increased at a very slow rate, and the head loss was recorded.

As the flow rate was increased, the column of insulation was compressed into a smaller and smaller length. The initial bed thickness of insulation ($l_0 = 7$ inches) was at a flow rate of $V = 0.1$ ft/sec and decreased to $l = 3.75$ inches at $V = 0.525$ ft/s. The increasing pressure on the column of insulation compressed the insulation by 46 percent of its original height. When the flow rate was returned to 0.0 ft/s the subsequent insulation bed thickness was only 5.5 inches. This apparent permanent compression from the initial bed thickness is the result of fiber fracture and reorientation which reduce the average void size. The head loss across the insulation structure is inversely related to the fiber diameter and strength. Since the cross-sectional area does not change during the experiment, the size of the voids must also have decreased by the same percentage. The void size decreases as the glass fibers fracture from the hydraulic forces, which are proportional to the fluid velocity at any given temperature.

The head loss results are shown in Table 3 under the column 6.0-u. A curve-fit to the data showed the head loss to be proportional to $V^{2.08}$, which is the largest

exponent measured for the velocity in any test. In comparison the preconditioned series A shreds had a smaller exponent on the velocity of 1.45. Thus, the compression of the insulation leads to increasing values of the exponents in the velocity term of the head loss equation. The smaller exponent of 1.45 on the velocity term confirms the pre-compression of the preconditioned shreds.

The sensitivity of the head loss to the water temperature is shown in Figure 8. A nominal thickness of 3" series A shreds were placed in the test facility, and the water temperature was gradually increased from 20 °C to 49 °C. There is a steady decrease in the head loss with increasing temperature. The head loss was found to decrease as $T^{-.540}$. Data published for the viscosity of water shows that it decreases like $T^{-.549}$, which indicates that the head loss is linearly related to the viscosity. Hence, the flow through the insulation can be considered to be laminar flow through a porous medium.

Taking the head loss to be dependent on the temperature, thickness and velocity, a new regression formula can be obtained, which would more closely approximate the conditions during a loss-of-coolant accident. The formula is listed at the bottom of table 5, and would be useful in situations where the accumulated debris has not been precompressed.

To determine if the characteristics of the insulation would change with time, a nominally 6 inch layer of series A shreds was placed in the test section of the pipe facility. The flow was allowed to run continuously for a long period of time, and the head loss was measured periodically. The head loss change over a period of 16 days is shown in Figure 9. Over the first couple of days the shreds were observed to become more compact on the screen. The "settling" of this material led to a measurable increase in the head loss. However, the rate of change continuously decreased, and after about 9 days the insulation did not show any significant changes. The increase in head loss for the aged insulation is similar to the effect of

preconditioning the samples. In both cases the size of the voids has been reduced, which leads to higher head loss.

The effect of an elevated pH level on the head loss across the thermal insulation was studied using a nominally 6 inch thick column of series A shreds. Borax was added to the flow until the pH level reached 9.5, which was determined with a Hanna pH meter. The head loss was measured at several different flow rates ranging from 0.1 to 0.5 ft/sec. Next the pH level was reduced to 8.5, and the head loss measurement repeated. This process was repeated for pH values ranging from 8.0 to 9.5. It was found that within the repeatability of the measurements the insulation was not affected by the pH level .

Tables 3 and 4 display the head loss values for the preconditioned test samples of series A and series B, respectively. This data is considered as baseline with respect to compression, fluid temperature considerations, time of exposure, and pH, recognizing compressibility is at the conservative extreme.

Table 3 Series-A Thermal Insulation

Measured Head Loss (ft of water)

Flow Speed (ft/s)	Material	T = 52°C Nominal Thickness (inches)							
		0.125	0.25	0.50	1.0	2.0	3.0	6.0	6.0-u*
0.1	shreds	.011	.027	.054	.168	.379	.609	1.19	.507
	Fragments	.002	.014	.030	.072	.260	.620	3.47	
	As Fabricated		.050	.058	.179	.558	1.15		
0.2	shreds	.025	.069	.151	.473	1.06	1.65	3.78	2.14
	Fragments	.008	.039	.097	.239	.794	1.69	7.65	
	As Fabricated		.145	.187	.536	1.58	3.17		
0.3	shreds	.042	.121	.273	.866	1.95	2.96	7.40	4.98
	Fragments	.018	.070	.194	.484	1.52	3.05	12.2	
	As Fabricated		.270	.373	1.02	2.90	5.76		
0.4	shreds	.059	.179	.417	1.33	2.99	4.48	11.9	9.06
	Fragments	.033	.106	.317	.799	2.42	4.63	16.9	
	As Fabricated		.419	.608	1.60	4.46	8.79		
0.5	shreds	.078	.243	.579	1.85	4.17	6.18	17.3	14.4
	Fragments	.053	.147	.463	1.18	3.47	6.39	21.8	
	As Fabricated		.589	.888	2.28	6.24	12.2		

*u - indicates the insulation was not preconditioned by having the air pressed out.

Table 4 Series-B Thermal Insulation

Measured Head Loss (ft of water)

Flow		T = 52 °C						
Speed	Material	Nominal Thickness (inches)						
(ft/s)		0.125	0.25	0.50	1.0	2.0	3.0	6.0
0.1	shreds	.045	.052	.095	.126	.269	.464	1.0
	Fragments	.005	.014	.029	.050	.146	.144	.794
	As Fabricated	.033	.050	.112	.335	.672	.744	
0.2	shreds	.088	.133	.238	.381	.777	1.32	3.11
	Fragments	.020	.052	.121	.188	.531	.565	2.44
	As Fabricated	.101	.161	.327	.865	1.87	2.16	
0.3	shreds	.130	.230	.408	.729	1.45	2.44	5.75
	Fragments	.048	.109	.280	.410	1.13	1.26	4.71
	As Fabricated	.193	.316	.610	1.51	3.42	4.04	
0.4	shreds	.172	.34	.6	1.16	2.24	3.77	8.91
	Fragments	.087	.186	.508	.712	1.93	2.21	7.51
	As Fabricated	.306	.511	.950	2.24	5.23	6.29	
0.5	shreds	.213	.46	.81	1.65	3.16	5.28	12.5
	Fragments	.135	.281	.807	1.09	2.92	3.44	10.8
	As Fabricated	.437	.742	1.34	3.04	7.27	8.87	

Multiple regression analysis was applied to the data presented in order to find the best fit of the data in Tables 3 and 4 to the equation $\Delta h = ae^{bv^c}$. The results are shown in Table 5.

Table 5 - Summary of Regression Coefficients

	Series A	Series B
Precondition Shreds	103 e ^{1.32} v ^{1.45}	72.0 e ^{.938} v ^{1.48}
Fragments	182 e ^{1.61} v ^{1.60}	67.7 e ^{1.13} v ^{1.91}
As-Fabricated	161 e ^{1.28} v ^{1.56}	123 e ^{1.03} v ^{1.53}
Uncondition Shreds	1285 T ^{-0.54} e ^{1.32} v ^{2.08}	

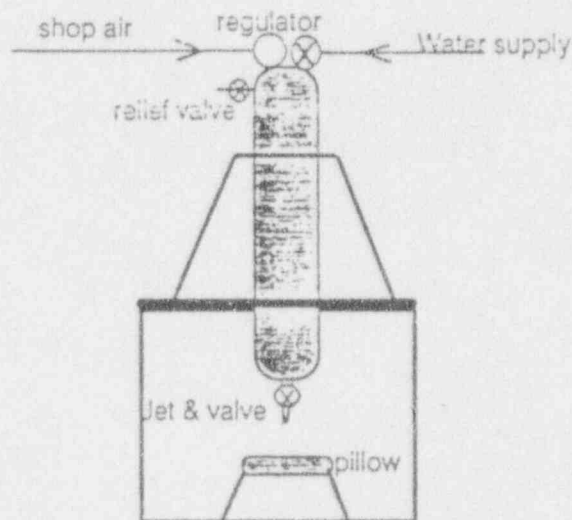
5.0 Jet Impact Test

The insulation placed around the pipes is covered with a fiberglass material in the form of pillows. If a pipe cracks at some point, then the pillow would be subjected to a high pressure stream of fluid. It is necessary to obtain some measure of the stagnation pressure of the fluid jet that would break through the cover and dislodge the insulation from the pillow. To simulate this process, a high pressure water jet facility was constructed.

5.1 Test Facility

An 8 inch diameter pipe, 48 inches long was capped at both ends and mounted vertically in a test stand as shown in the figure below. The top of the pipe was connected to a regulator and high pressure supply of air. A valve connected to a water line supplied water to the pipe, and a pressure gauge measured the interior

stagnation pressure. A valve and 1/4 inch diameter jet were positioned at the bottom of the pipe. The valve could be opened quickly to start the jet almost instantaneously. The pillows were placed 7 inches below the exit of the jet, and were tested at both a 90° and a 45° angle with respect to the jet.



5.2 Results

Tests were conducted on pillow type TW-A1-2 and TW-B1-2. Both showed similar behavior. Each test consisted of a 5 second exposure of the pillow to the water stream. The streams formed a 1/8" x 3/4" oval region of impact on the pillow.

With the pillows oriented perpendicular to the jet noticeable damage to the fibers began at a stagnation pressure of 30 psig. The fibers began to separate in the weave. Between 60 psig and 100 psig the fibers turned white, and a sizable dent appeared in the cover, but the jet did not break through the material. With a 100 psig exposure to the jet stream the jet required between 45 - 60 seconds of exposure before it broke through the cover.

When the pillows were oriented at 45° to the jet, there appeared to be less damage to the cover than when it was perpendicular to the jet. However, the 100 psig jet was able to break through the cover after a 30 second exposure. When the jet impacted the pillow at an oblique angle, the fibers in the cover tended to spread apart more rapidly than when the jet was perpendicular to the cover. This may explain the reason why it took less time for the 45° jet to break through the cover.

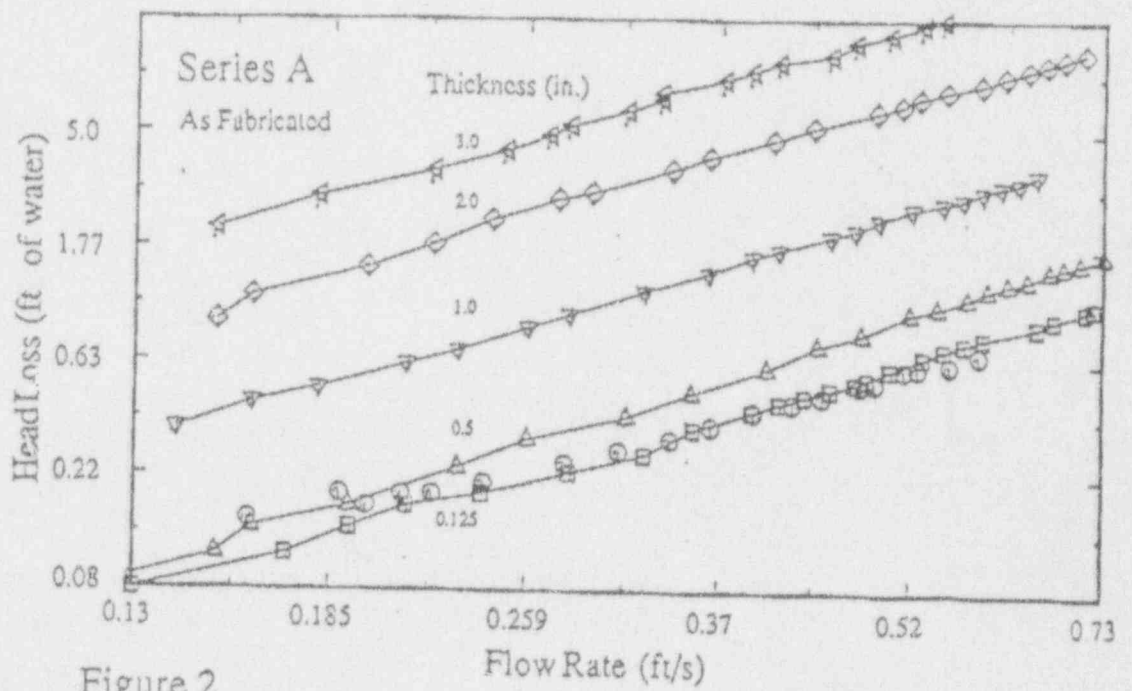
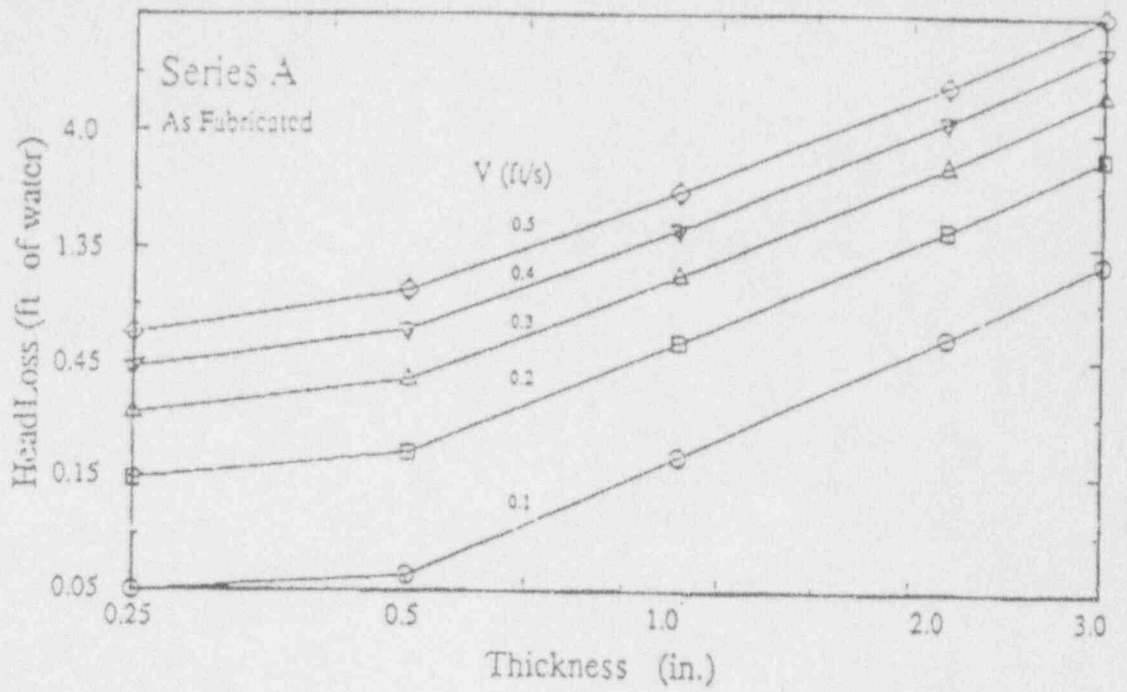


Figure 2

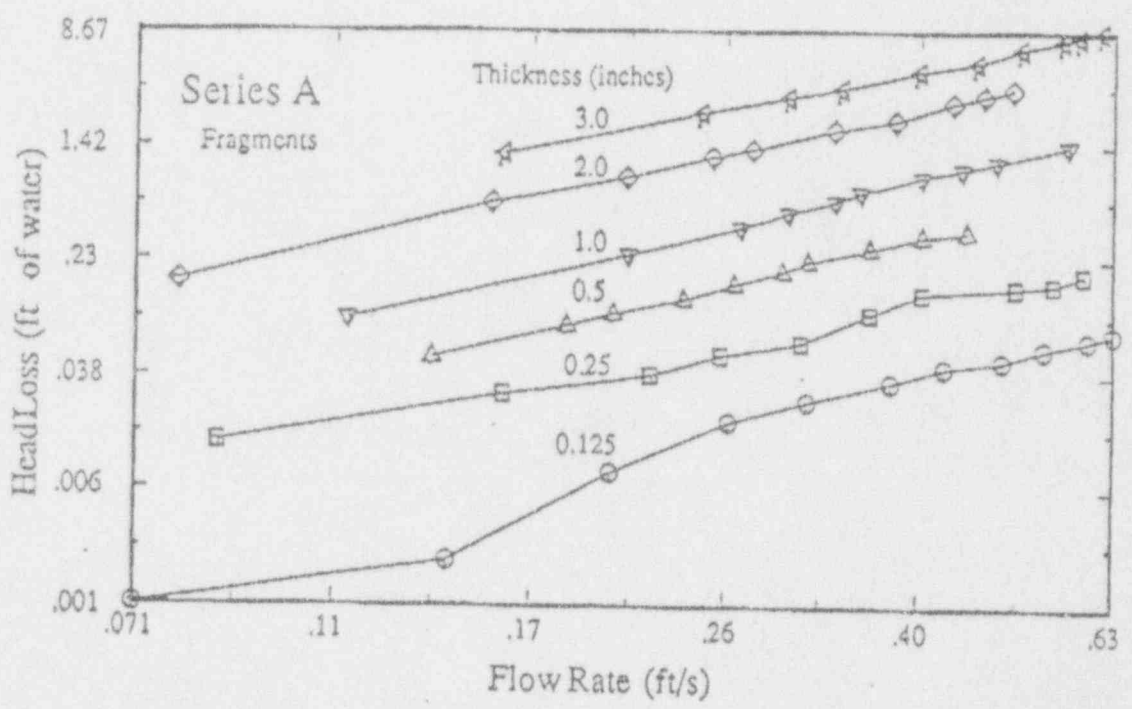
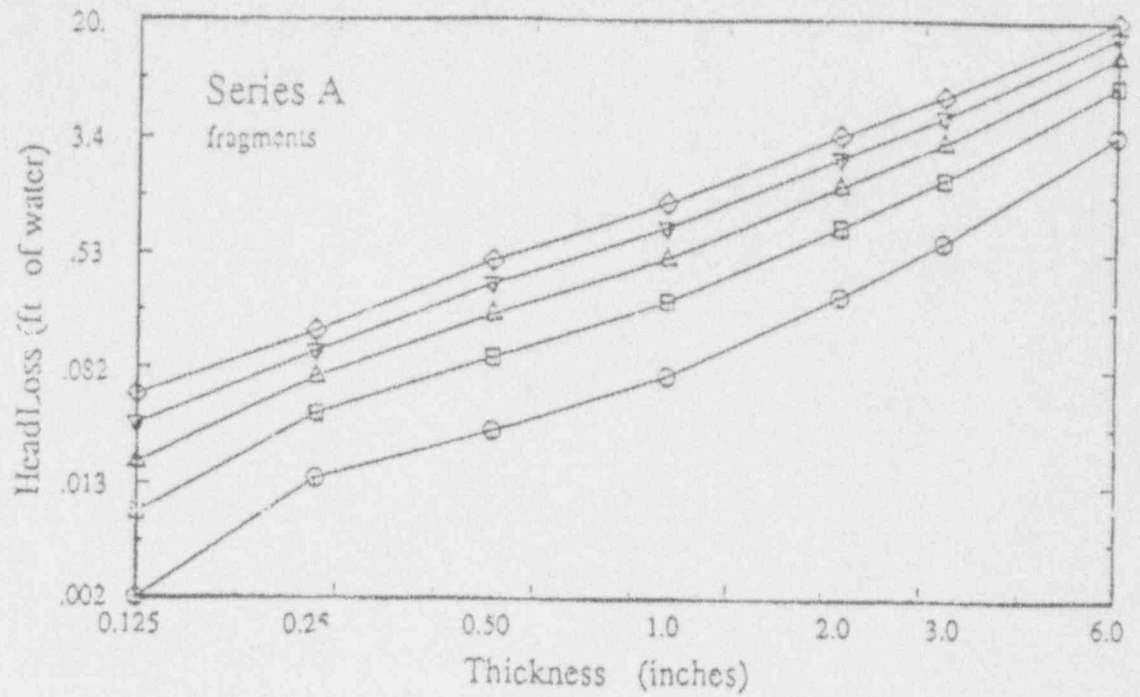


Figure 3

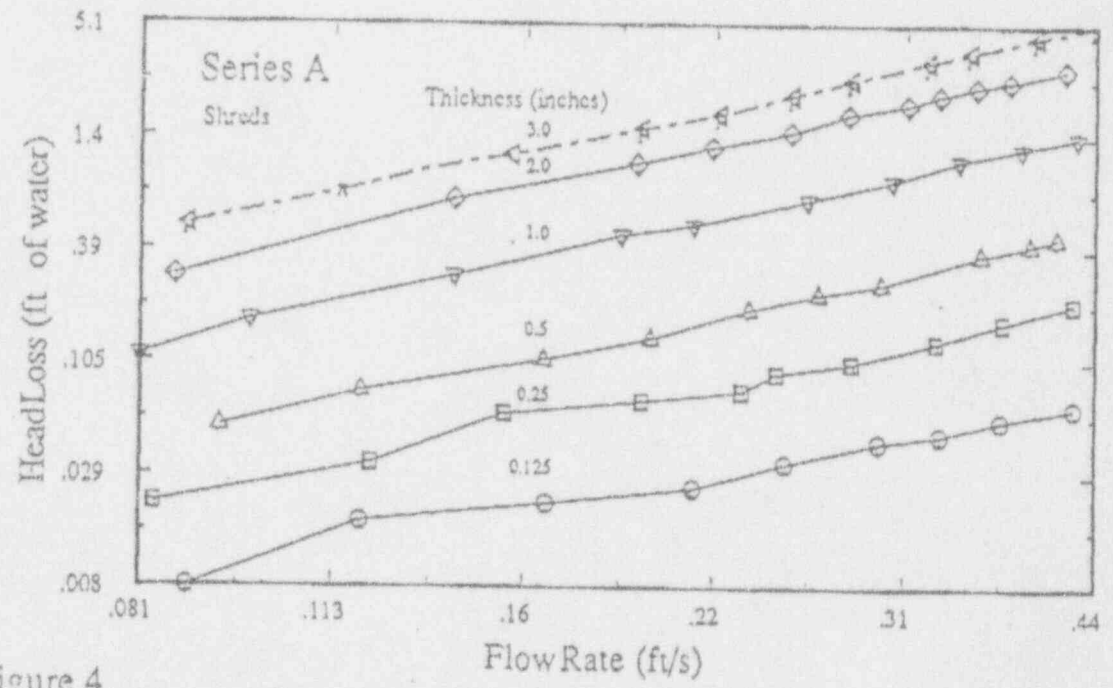
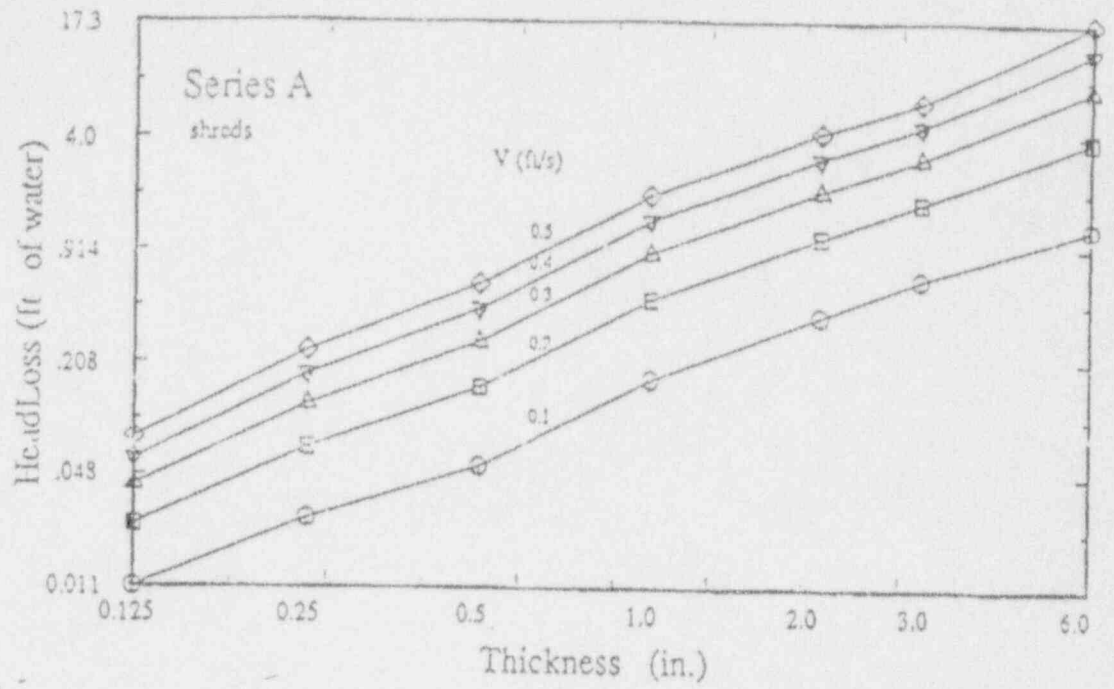


Figure 4

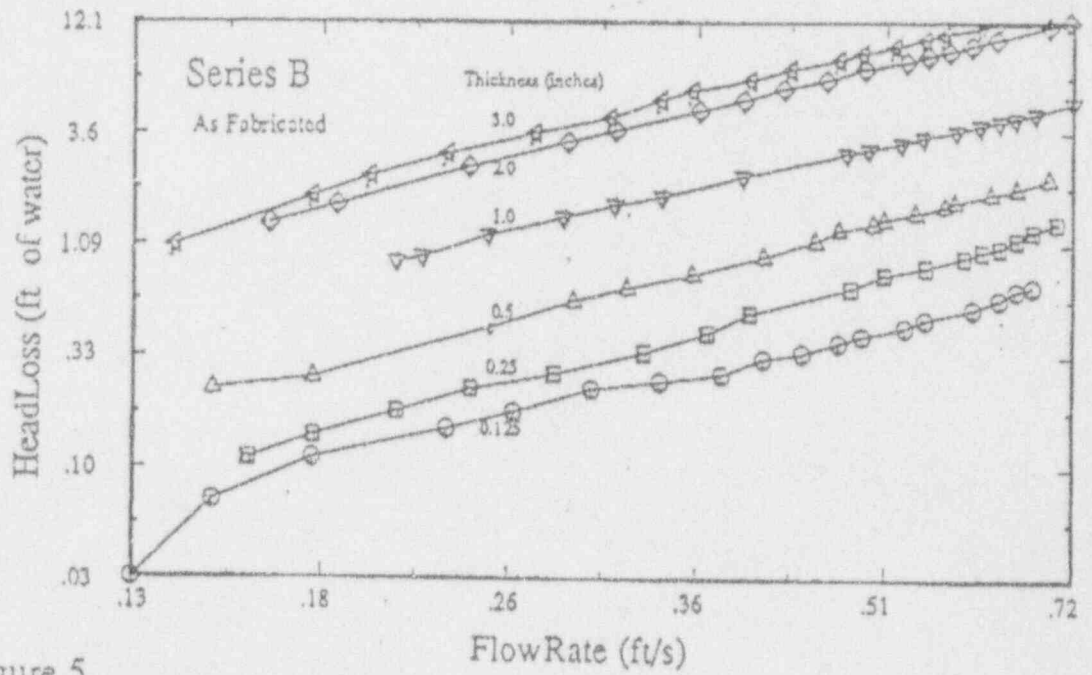
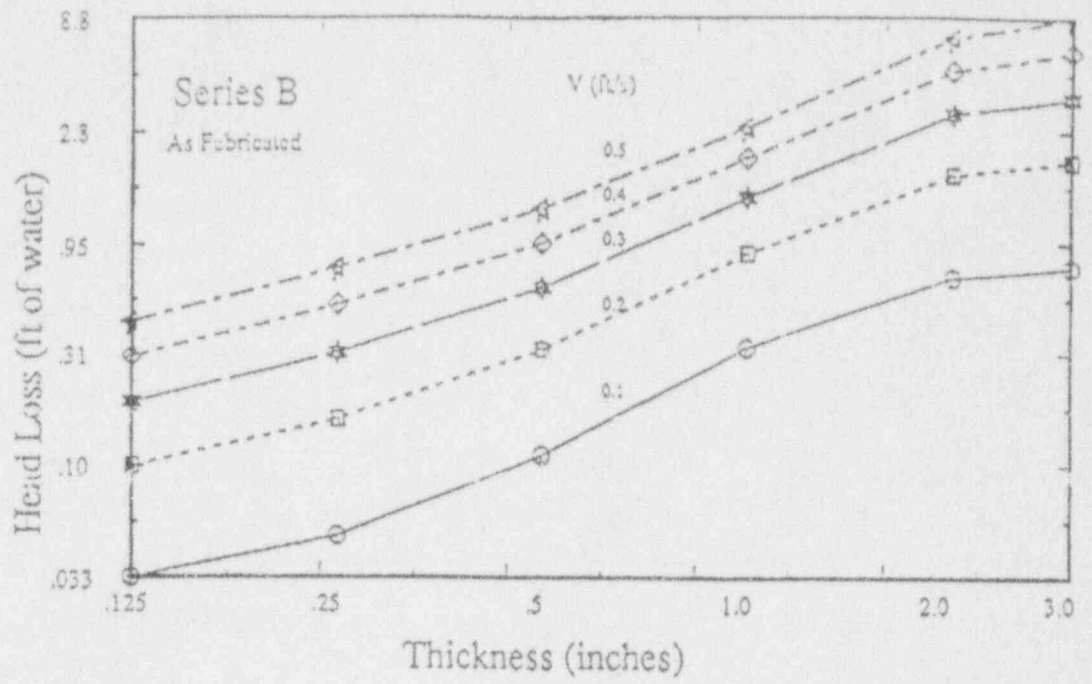


Figure 5

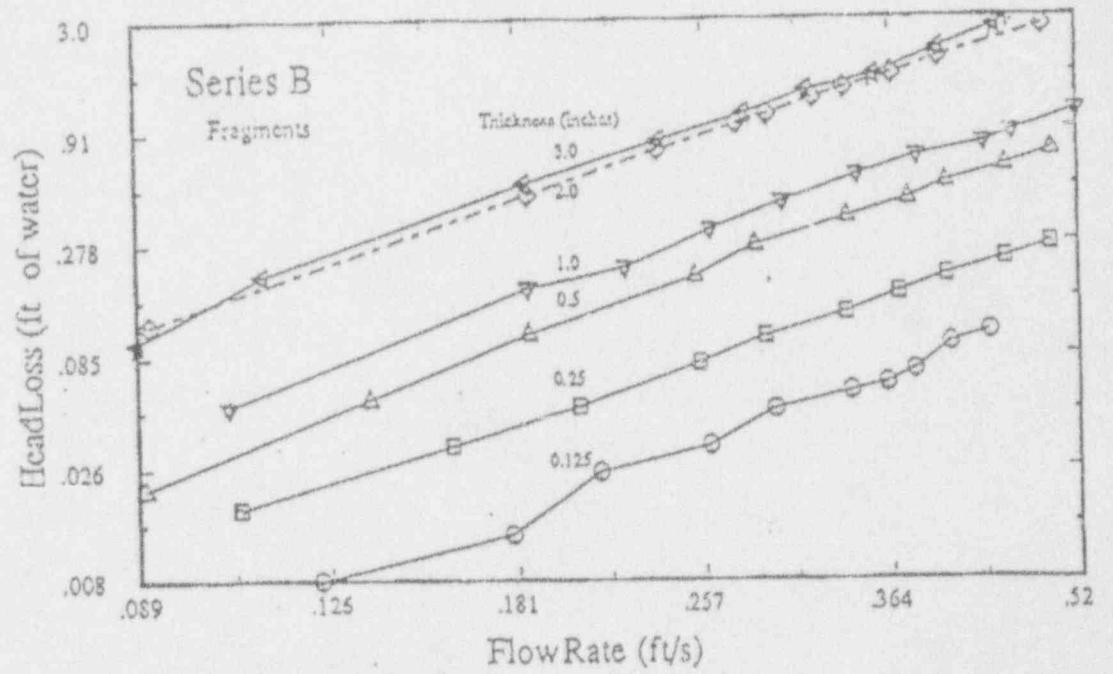
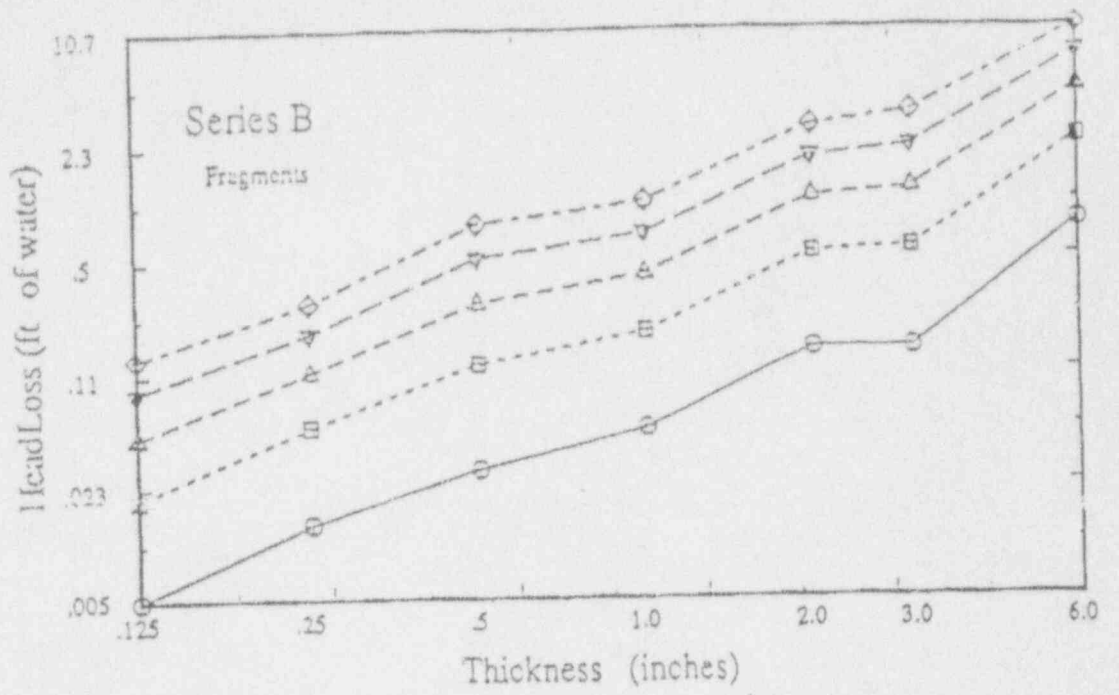


Figure 6

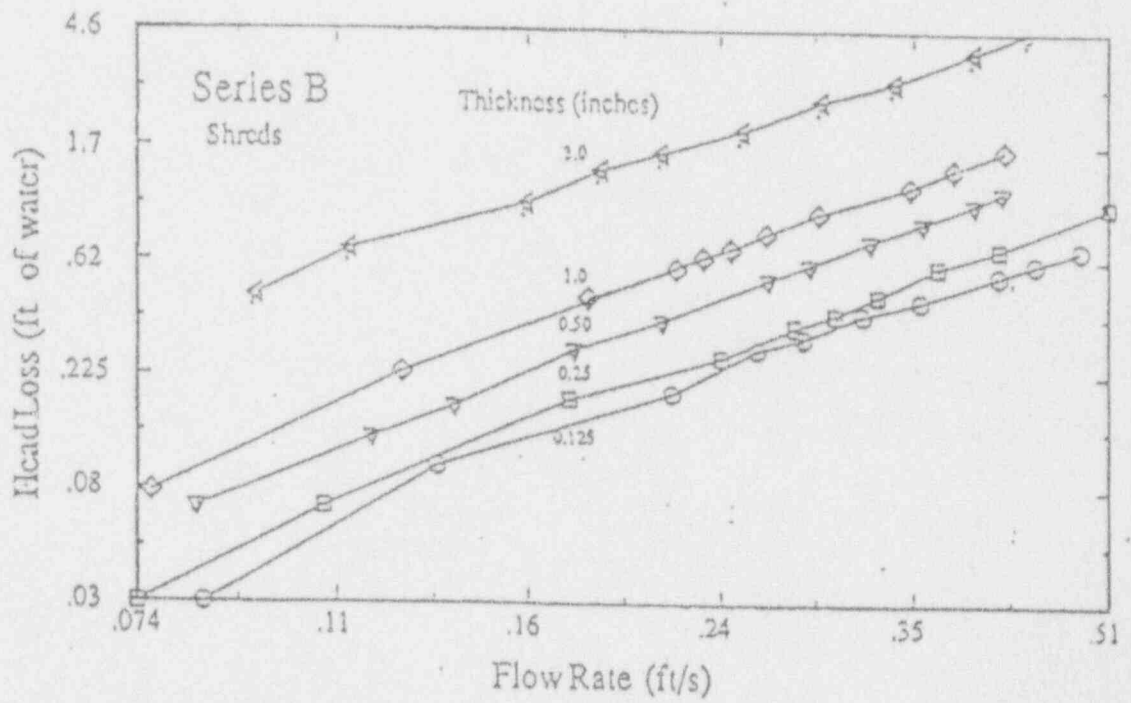
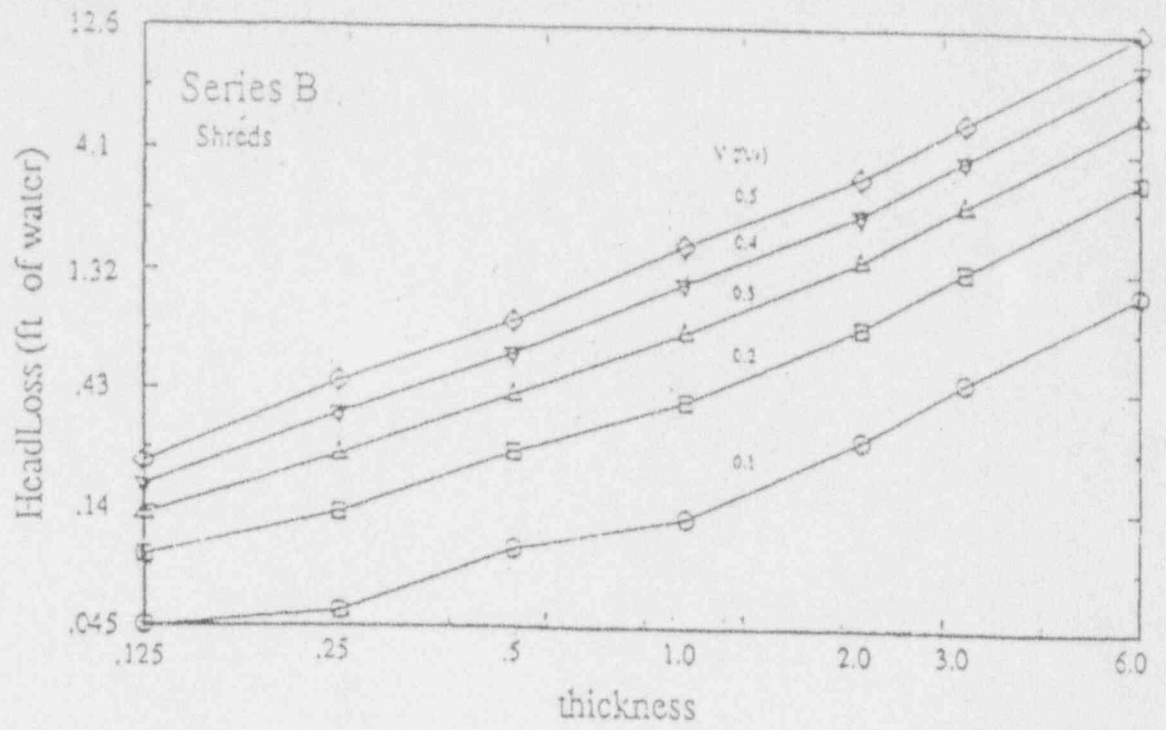


Figure 7

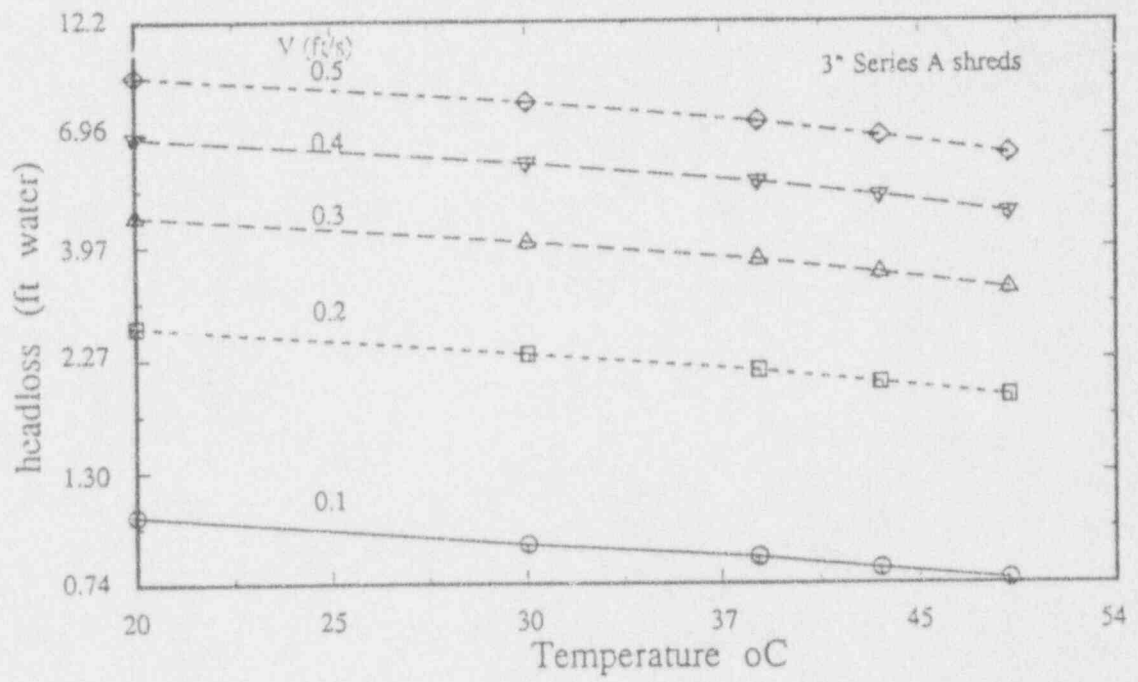


Figure 8

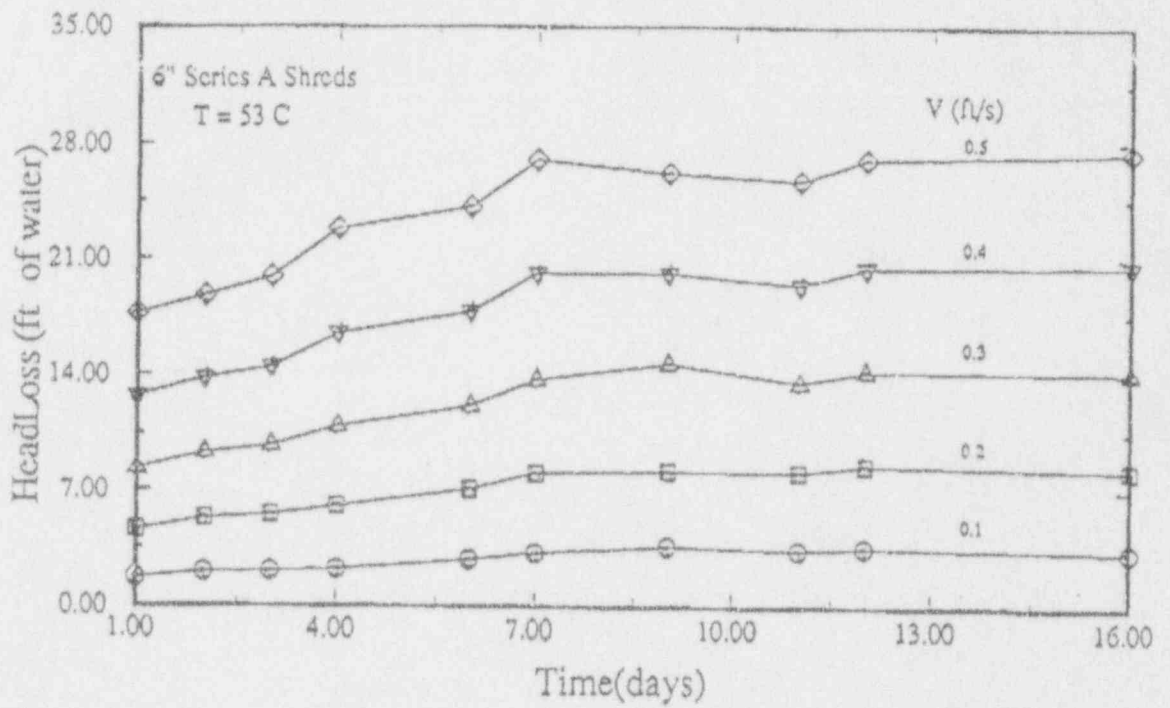


Figure 9